

# **JOURNAL OF KUFA-PHYSICS**

journal.uokufa.edu.iq/index.php/jkp/index | ISSN: 2077–5830



# Studying the effect of annealing time on structural, morphological and optical properties for AZO nanostructures

Zainab Saad Lafta<sup>1</sup>, Hayder J. Al-Asedy<sup>1\*</sup>

<sup>1</sup>Physics Department, Faculty of Education, University of Al-Qadisiyah, Diwaniyah, Iraq

\*Corresponding Author E-mail: phy.edu.post33@qu.edu.iq hayder jawaad@yahoo.com

### ARTICLE INF.

# Article history:

Received: 23 DEC, 2024 Revised: 13 MAR., 2025 Accepted: 21 APR., 2025 Available Online: 28 JUN.

2025

# Keywords:

AZO nanostructures:

Spin coating;

Time annealing

Structural properties; Morphological properties

#### ABSTRACT

ZnO:Al films with a 1% Al/Zn atomic ratio were created using a sol-gel spin coating technique on glass substrates. The films were annealed for a duration ranging from 2:20 to 3.40 hrs. at 500 °C. The effects of annealing time on the structural and morphological properties of AZO films were investigated utilizing X-ray diffraction (XRD), SEM and EDX to characterize samples. Scanning electron microscopy analysis showed that ZnO nanostructures with varying average sizes were developed for both as-deposited samples and annealed films. SEM revealed that both the number and size of nanosheets increased. The EDX patterns showed the right elemental traces and the oxygen ratio-mediated growth of the ZnO nanostructure on the glass substrate was visible in EDX patterns. By measuring the absorbance and transmittance spectra in the wavelength range (300-850 nm), the optical characteristics were obtained. It was found that as annealing time increases, absorbance reduces while transmission increases. The optical measurements revealed the type of transition that was a direct allowed with an average band gap energies lie between 3.76 eV and 3.12 eV with the rising of annealing time.

DOI: https://doi.org/10.31257/2018/JKP/2025/v17.i01.18254

# دراسة تأثير زمن التلدين على الخصائص البنيوية والشكلية والبصرية لهياكل النانو AZO

زينب سعد لفته، حيدر جواد الاسدى \*

قسم الفيزياء، كلية التربية، جامعة القادسية، الديوانية، العراق

# الكلمات المفتاحية:

الخلصة

هياكل نانوية من AZO، الطلاء بالدوران، الركيزة الزجاجية،

في هذه الدارسة تم تحضير أغشية رقيقة من أوكسيد الزنك النانوي المشوب بالألمنيوم (AZO) بنسبة (1%) ، بطريقة المحلول الجيلاتيني (sol-gel) وترسيبها بتقنية الطلاء الدوراني (spin) coating) على ركائز زجاجية، و تم تلدين الأفلام لمدة تتراوح بين (2.20-3.40) hr عند(0°C أ

زمن التلدين، الخصائص الهيكلية، الخصائص المور فولوجية. ، كما تم دراسة تأثير زمن التلدين على الخواص الهيكلية والتركيبية لأغشية AZO باستخدام حيود الأشعة السينية (XRD)، SEM وEDX ، أظهر تحليل المجهر الإلكتروني الماسح أنه تم تطوير هياكل نانوية من أكسيد الزنك بأحجام متوسطة ومتفاوتة لكل من العينات الغير ملدنة والملدنة بأزمان تلدين مختلفة، وتمت دراسة الخصائص التركيبية للأغشية بواسطة المجهر الالكتروني الماسح (SEM)، حيث وجد أن عدد وحجم الجسيمات النانوية قد زاد بزيادة زمن التلدين، كما أظهرت أنماط (EDX) تطوراً لبنى (AZO) النانوية على الركائز الزجاجية. وبقياس طيف الامتصاصية والنفاذية ولمدى الاطوال الموجية mn (850-850)، تم الحصول على الخصائص البصرية وقد وجد أنه مع زيادة زمن التلدين، تقل الامتصاصية بينما تزداد النفاذية. وتكشف القياسات البصرية عن نوع الانتقال الذي كان مسموحا به بشكل مباشر عند فجوة الطاقة ويتراوح بين 3.76 eV 3.12 eV مع زيادة زمن التلدين.

#### 1. INTRODUCTION

ZnO nanostructures have recently gained significant attention because of their unique characteristics, namely their large band gaps (3.37 eV), which regarded natural n-type semiconductor Additionally, materials[1]. ZnO nanostructures have a high excitation binding energy of 60 mV at ambient temperature, which is higher than the energy of any other materials[2].Its high resistivity, medium dielectric constant, high heat capacity, high thermal conductivity, and low water absorption draw a maked study interest. ZnO is a substance and it can be produced in a number of nanostructures with ease [3,4]. Zinc oxide absorbs UV light with a wavelength less than 380 nm and is transparent to visible light [5]. The ZnO thin films are important for technology because of their diverse spectrum of optical and electrical characteristics [6]. Transparency, great abundance, nontoxicity, exceptional chemical and mechanical durability are only a few of the benefits that ZnO thin films offer over other oxide thin films such as ITO, CdO, SnO2, etc. The Zinc oxide thin films, often known as transparent conductive oxides, are a common component of solar cells, furthermore, it can serve as gas sensors and piezoelectric devices.

In order to manufacture ZnO films of superior quality, a variety of techniques have been utilized. These methods include the sol-gel method, radio frequency magnetron sputtering, chemical vapor deposition, atomic layer deposition, pulsed laser deposition, and plasma-assisted molecular epitaxy [7-12]. The sol-gel chemical deposition process is particularly appealing among them because it is simple to use in the laboratory to create semiconducting thin films. With this method, ZnO thin films can be inexpensively coated on big and tiny use in technological areas for applications [13-16], quick chemical reaction times. non-vacuum environment, and low temperature productivity less than 100 °C [17]. Not only can growth techniques affect ZnO film characteristics, but post-growth treatments like thermal annealing also have an impact. The influence that annealing has on the characteristics of ZnO thin films has been documented by a number of different groups [13-16].

The findings, especially concerning the influence of annealing duration on the structural and optoelectrical characteristics of ZnO:Al films, remain contentious. However, there were differences across the groups in the annealing parameters, such as the

temperature, time, and ambient gas species.

In this study, ZnO:A1 nanostructures created on glass substrate with different annealing times annealing for(2:20-3.40) hr at temperature of 500 °C, taking into account the noteworthy benefits of the combined sol-gel and spin coating approach. thus, prepared nano film samples and studying their structural, morphological and optical characteristics are identified as a function of annealing time.

# Experimental details 2.

ZnO:Al nanofilms were deposited onto glass substrates using the spin coating and sol-gel techniques. As a starting material, Zinc acetate dihydrate (ZnAc) [Zn (CH3COO).2H2O] (Alfa Aesar, 99.999 percent), the dopant source of aluminum is the aluminum nitrate nonahydrate [Al (NO3)3·9H2O] diethanolamine (DEA) were dissolved in 2-propanol (C3H8O) at a concentration of 0.1 M. (AR, Merck). A transparent and stable solution was then obtained by adding DEA after using 2propanol, (ZnAc), and DEA as the solvent and stabilizer, respectively. ZnAc and DEA were kept at a 1:1 molar ratio in the solution, which is shaked with a magnetic stirrer at 65 °C for 90 minutes. After 24 hours, a clear, homogeneous solution was produced, which is subsequently spin-coated onto glass substrates. The complete coating and drying procedure occur over 35 seconds at 3000 rpm. The films were subjected to drying in an oven at 220 °C for 10 minutes following deposition. Ten times of coating and drying were

completed to reach to the required thicknesses. The obtained AZO nanostructured films (as prepared) and annealed at 2.20, 2.40, 3.00, 3.20, and 3.40 h in a microprocessor-controlled furnace 500 °C at a heating rate of 5°C/min. X-ray diffraction (XRD, Bruker D8 Advance Diffractometer) was used to describe the morphology structure of (all) produced materials. Cu-Kα radiations (1.5406) A° were used, and the scanning range (2) is 20-80°. The scanning is done at a modest rate of 1.2°/min. The elemental composition was assessed by an energy dispersive X-ray diffractometer (EDX), whereas surface morphology optical qualities were evaluated using a scanning electron microscope (SEM, ZEISS SUPRA 35 VP).

### 3. Results and discussion

## 3.1 Structural Properties:

# 3.1.1 X-Ray Diffraction (XRD)

The XRD pattern of pre-annealed and post-annealed AZO nanofilm samples is illustrated in Figure 1. The samples are highly crystalline, evidenced by the clear visibility of sharp diffraction peaks. All samples exhibit peaks corresponding to the lattice planes (growth directions) of (100), (002), (101), (102), (110), (103), and (200) orientations, which align with the angular positions of 31.86°, 34.42°, 36.28°, 47.68°, 56.53°, and 62.92°, respectively. When compared to the normal JCPDS Card no. (36-1451) of ZnO with all the samples, hexagonal wurtzite polycrystalline structures can be seen. The observed rise in XRD intensity for the three highest samples with peaks (100), (002), and (101)

suggests preferential growth direction along the a or c lattice plane axes and both. The influence of size restriction is demonstrated by the fact that the full width at half maximum (FWHM) of these peaks decreases as the annealing time increases.

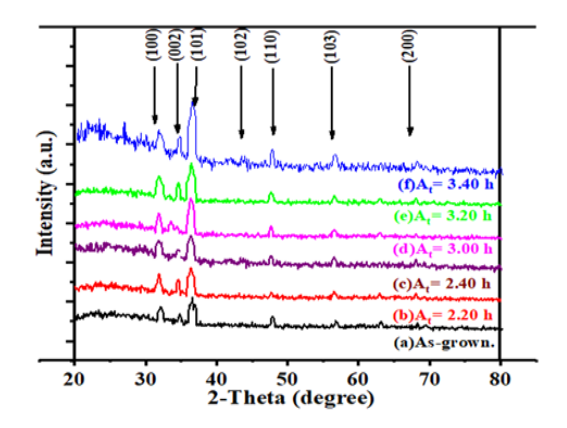


**Figure 1**. XRD pattern for prepared and post annealed at different annealing time samples.

Scherrer's equation was used to calculate the crystallite size (D) of the nanocrystallites:

$$D_{av} = \frac{k\lambda}{\beta\cos\theta} \tag{1}$$

Where  $\lambda$  is the wavelength of incident X-ray from XRD,  $\beta$  is the FWHM measured in radians and  $\theta$  is the Bragg angle of diffraction peak. As the annealing duration extended from 2.20 to 3.40 hours, while maintaining a

constant temperature of 500 °C, the grain sizes increased, hence enhancing the crystallinity of the nanofilms. Controlling the annealing period allows for an improvement in the crystalline quality of the films [18]. The rapid reduction of non-bridging oxygen type defects and the resultant enhancement in the formation of ZnO grains are attributable to the modifications in nanofilm growth facilitated by this annealing duration [19]. As measured by the length of the dislocation lines per unit volume of crystal, the dislocation density  $(\delta)$  shows a decreasing tendency as annealing time increase. As a result, there are fewer lattice defects overall. For this film, we use the dislocation density formula by Williamson and Smallman [20], as listed in Table 1, and. D and FWHM values both went up, indicating that the nanostructured ZnO thin films crystallized better. The projected AZO NSs' estimated (c/a) ratio matched that of the ZnO bulk crystal's JCPDS Card No. 36-1451[21].

**Table 1** Annealing time dependent variation of FWHM, grain size, lattice parameters (a &c) with (c/a) ratio, Volume and dislocation density

Ta/(hr)	β×10 <sup>-3</sup> /	D/(nm)	a(Å)	c(Å)	c/a	$V/(\mathring{A})^3$	$\delta/(nm^{-2})$
	(Rad)						
0.00	0.721	15.32	3.2497	5.2064	1.6021	47.614	0.00426
2.20	0.601	16.73	3.2502	5.2061	1.6017	47.629	0.00357
2.40	0.517	18.46	3.2511	5.2052	1.6011	47.644	0.00293
3.00	0.428	21.31	3.2515	5.2043	1.6006	47.648	0.00220
3.20	0.318	27.46	3.2521	5.2034	1.6001	47.657	0.00132
3.40	0.246	34.77	3.2525	5.2032	1.5997	47.667	0.00082

With longer annealing times, there was a noticeable shift in the (101) peak position toward a lower diffraction angle (Table 1), indicating that macroscopic strain had changed the lattice parameter (cell volume increasing lead to shifted towards smaller angle), that mean, a left-handed shift in X-ray diffraction pattern signifies lattice relaxation, while a right-handed shift corroborates the presence of a strained lattice. In contrast to the standard, all of the peaks have shifted to a lower  $2\theta$  value and have broadened (for a shorter annealing period. Defects in ZnO:Al thin films, including oxygen vacancies and lattice disorders, are during the annealing process, resulting in significant lattice shrinkage [22]. The grain size of the asprepared sample (0.00 hr) was 15.32 nm, which increased to 21.31, 27.46, and 34.77 nm after 3.00, 3.20, and 3.40 h of annealing time, respectively. This showed that the crystalline quality of film improved with longer the annealing times. Prolonged annealing time resulted in granule expansion and a reduction in nonbridging oxygen defects, hence facilitating the formation of ZnO grains [21]. Increasing the annealing time has also shown to improve the overall crystallinity of AZO NSs films. Additionally, we can

see that as time increases, crystallite size increases.

The predicted grain size's temperature-dependent change is summarized in Table 2, strain, stress and density that is calculated from the equation. 1 [22].

$$V = 0.866a^2c$$
 (2)

where a,c are lattice constants. It was also noted that when the annealing time increases, the density decreases. This is because of increasing in volume (a& c), and higher D when highly crystalline ZnO nanoparticles, cation and anion vacancies, stretched defects such dislocations, etc. are presented in the nanostructures utilized in these applications.

The overall film topologies were significantly altered as a result of the annealing temperature-induced lattice relaxation, which was influenced by the different dangling bonds within the film. The electrostatic interaction between the oxygen ions adsorbed from the surrounding environment and the dangling bonds on the AZO surface is responsible for a portion of the lattice shrinkage.

Table 2 Annealing time dependent Grain size, Strain, Stress, Energy band gap and density for AZO nano film samples.

Annealin g time (hr)	Grain size (nm)	Strain (ε)	Stress(σ) /(MPa)	Energy band gap/(eV)	ρ(gm/cm <sup>3</sup> )
0.00	15.32	-0.000507	1.18	3.76	5.6395
2.20	16.73	-0.00107	2.49	3.46	5.6377
2.40	18.46	-0.00276	6.43	3.40	5.6359
3.00	21.31	-0.00445	10.4	3.30	5.6355
3.20	27.46	-0.00614	14.3	3.22	5.6343
3.40	34.77	-0.0191	44.4	3.12	5.6403

Table 2 shows the predicted annealing time dependent values for all the strain and stress along the samples of generated ZnO:Al thin films. Negative strain readings indicated compressive properties. The strain values in this analysis are found to be negative (compressive in nature). Although there may be some extrinsic residual tension in the structure of the films (due to long thermal annealing times), there is also a sizable amount of intrinsic stress. For these samples (the stress with positive sign), The computed stress for each of the films had a positive sign, indicating that  $(c_0>c)$ ; as a result, the crystallites under extensional Additionally, this stress is marginally lessened when the annealing time rises, suggesting that the appropriate in an annealing time did not cause the crystal structure to be significantly deformed [22]. Is classified into two categories: extrinsic, resulting from the disparity in thermal expansion coefficients between the film and substrate, and intrinsic, arising from impurities, defects, and lattice distortions inside the crystal [23].

The XRD study and increased grain size with extended annealing times were matched. As the annealing time increases, the average diameter of the NPs grows because the aggregation of NPs, prompted by thermal energy, causes the time extension. Decreased nobridging oxygen flaws and the subsequent beneficial creation of a hexagonal structure may also have contributed to the enhanced morphology [24].

# 3.2 Morphological Properties of ZnO:Al nanostructures:

The compositional study of AZO nanofilms has been conducted utilizing SEM images. The raster region has been used to analyze the depth profile spectra of ZnO thin films, both as-grown and after annealing. Figure 2 (a), (c), (e), (g), (i), and (k) presents SEM images (top view) of AZO nanofilm samples, encompassing both pre-existing and synthesized samples subjected annealing durations of 0.00, 2.20, 2.40, 3.00, 3.20, and 3.40 hours, respectively. All samples, with the exception of the as-prepared sample, contain a mixture of nanoparticles and nanosheets. In contrast, the sample that had not been annealed had a uniform surface with a high grain density and higher nanoporous features as show in Figure. 2 (a) (many big white spots). It was clearly observed that the no annealing time nificantly affected on the surface morphology of the AZO thin films (just pre-heating).

Nevertheless, samples that were annealed for 2.20 hours (Figure. 2 (c)) and for 2.40 hrs (Figure. 2 (e)) have different surface morphologies somewhat different. This is due to the fact that the annealing process supplied enough thermal energy for formation of such nanostructures (NPs and NSs). For the samples (c&e), the nanostructure of the two samples is composed of many spherical-shaped structures resembling particles [25].

The top view of the samples also showed a general rise in the regularity of the NPs, which were primarily composed of small amounts of big perpendicular nanosheets particles white in color in the Figures. 2 (g & i). Extending the annealing duration to 3.00 hours enhanced the crystallization of AZO nanostructures, leading to a rise in both the size and number density of

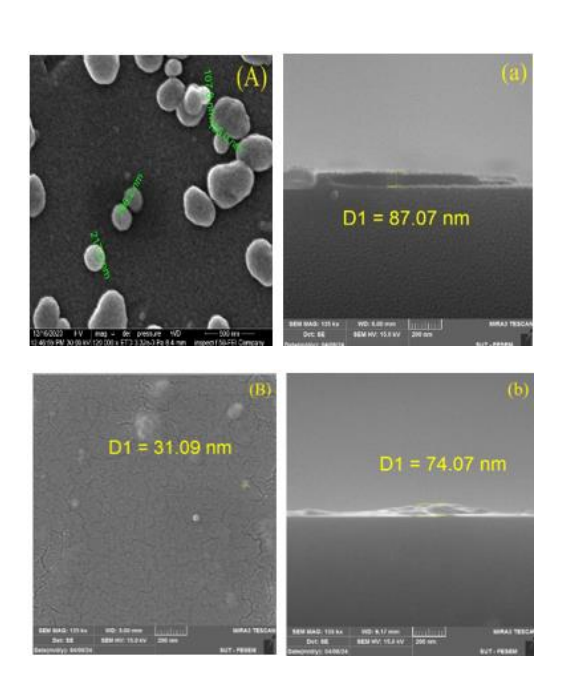
nanoparticles and nanosheets. It has been found that NPs' sizes range from 20 to 40 nm. On the NPs, some nanosheet were similar as can be seen in Figure. 2 (e & g) except that in the sample (g) where we noticed the appearance of more particles with increasing annealing time, and in terms of the clarity and prominence of a number of particles in a regular agglomeration, the sample (i) showed some spots in the form of aggregation, in addition to the agglomeration that already presented in it [22].

When the annealing time was increased to 3.40 h, (Figure. 2 (k)) the films seemed smooth and even, whereas the granules increased in size, became tightly compacted, and were uniformly dispersed. The particle size of the coatings increased with prolonged annealing time, as evidenced by prior XRD measurements [26,27].

The cross-sectional SEM images of the 0.00, 2.20, 2.40, 3.00, 3.20 and 3.40 hr annealed samples are shown in Figures 2 (b), (d), (f), (h), (j) and (l), respectively. Through thorough examination of the whole film cross-section, the thickness uniformity over a sizable portion of the substrate was confirmed (Figure. 2 (b)). The thin film

surface of the sample is absolutely free of any broken particles, and as there has not been any annealing, there were not any perpendicular nanosheets to be seen. The production of dense nanosheets with an estimated length of 74 nm was, however, clearly visible in the ZnO:Al NSs after 2.20 hour of annealing (Figure. 2 (d)). The development rate of nanosheets has been noticeably accelerated by a further extension of the annealing time 2.40 hrs (Figure. 2 (f)). It was also clear from the cross-sectional morphology of the sample after 3.20 hrs of annealing (Figure. 2 (j)) that thick and dense grains had grown on the edge glass substrate. The presence of some granules that are perpendicular to the surface of the substrate is indicated by the growth of huge crystallites with enhanced roughness (micro sheets) and with low roughness (nano another sheets), which were detected. The explanation for how nanosheets with ZnO:Al embedded formed together with nanoparticles, is because of the reaction of precursors materails to form ZnO:Al nuclei in the sol-gel assisted spin coating process. These kinds of nanostructures were produced as a result of rotation and the creation of uneven layers of unequal thickness (agglomerates of multiple complicated nanoparticles). The reaction process significantly also contributed the variety morphology of AZO nanostructures. On the other hand, oxidation at the higher time of about 3.40 h annealing period led to the development of nanosheets with a gradually rising density. At greater thickness, it is thought that the top oxide layer's

positive stress will grow significantly. It was resulting in a higher number of deformations and a quicker nucleation rate. As a consequence of an increase in annealing time, the oxidation duration increased, resulting in stress-induced nanosheets. For the annealed samples, the estimated grain sizes were greater than for non-annealed samples. It is obvious that as the synthesis time increases, so do the anticipated grain sizes.



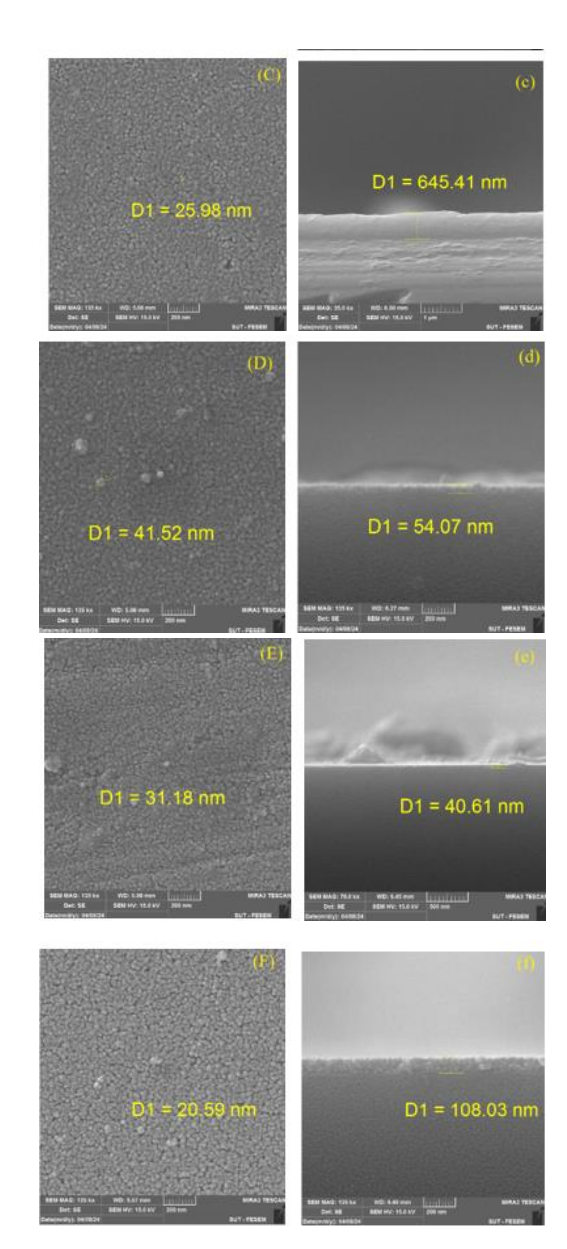


**Figure 2.** SEM images (top view) of AZO nanofilms: (a) as-prepared and annealed for (c) 2.20, (e) 2.40 (g) 3.00 (i) 3.20 and (k) 3.40 hr. on the left, the cross-sectional SEM images of samples: (b) as-prepared and annealed for (d) 2.20, (f) 2.40, (h) 3.00, (j) 3.20 and (l) 3.40 hr.

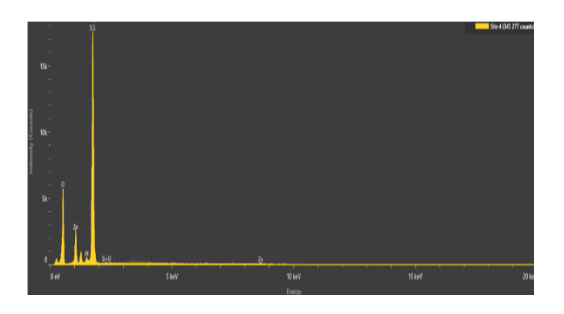
### 3.3 EDX results:

Figure. 3 demonstrates the EDX spectra of the ZnO:Al nanostructures sample at annealing temperature of 500 °C with annealing time 3.40 hrs, Which revealed the relative elemental

compositions of a portion of the sample studied containing chemicals such as Zn, O, Al and SiO2. It was found that the numbers which were computed for the atomic and weight percent of the elements were in excellent agreement with the values that were determined through experimentation.

The EDX results indicated that the crystalline nanomaterial had high ZnO values and produced lower intensity ratios for ZnO than those obtained by heat treatment of other samples. Furthermore, the intensity of the highest peak (101) correlated to the high annealing time at XRD Figure (1). It asserted that the higher level thermal annealing led to a substantial increase in crystallization and a robust lattice orientation of the ZnO:Al phase. This was accompanied by the formation of a significant number of oxygen vacancies. The 240minute annealing sample exhibited significantly more Znelemental peaks than the other samples, and the absence of any additional SiO2elemental peaks suggests that the sample is highly pure. This comparable to stoichiometric ZnO. No impurity elements were detected [28].

Furthermore, the oxygen elemental percentage as determined by EDX measurement was clearly affected by the annealing duration.



**Figure 3**. The EDX spectra of the ZnO:Al NS prepared with 500 °C at 3.40 hr.

## 3.4 Optical properties

### 3.4.1 Absorbance

**Figure** (4) illustrates the absorbance spectrum as a function of wavelength within the range of (300-850) nm, derived from the ultraviolet and visible regions of (AZO NS) compounds after the annealing for various durations (0.00, 2.20, 2.40, 3.00, 3.20, 3.40) hrs at 500°C. The spectra indicate that the nano samples significant absorption ultraviolet radiation in the range of 300-850 nm, while demonstrating minimal absorption in the visible and nearinfrared regions. Furthermore, it was observed that absorbance decreases progressively with increasing wavelength (for the only one curve), the absorbance increased with increasing the time annealing for all films, with the highest absorbance values occurring at shorter wavelengths. Due to the fact that the energy of the incident photon is lower than the optical energy gap of the semiconductor, this indicates that the photon that is incident on the electron does not possess sufficient energy to excite the electron and make it easier for it to transit from the valence band to the conduction band. The absorbance progressively diminishes with extended annealing time as the quantity of photons absorbed by the atoms increases [24,29,30].

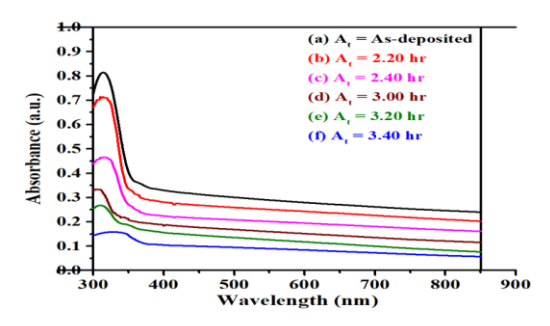


**Figure.3** The absorption spectrum of aluminum-doped zinc oxide Nano films annealed with different annealing times.

The peak absorption with red shift results with increased the annealing time, from the movement of electrons from the valence band to the conduction (O2p-Zn3d)in which absorption gap is less than 400 nm. The transfer and alteration in the energy gap may be attributed to grain size, potentially resulting from the enlargement of (AZO) crystals due to prolonged annealing or grain development, as well as modifications in the nanostructures. [31].

#### 3.4.2 Transmittance

The transmittance spectrum was analyzed within the wavelength range of 300-850 nm, as depicted in Figure (5). A maximum transmittance of approximately 91% was observed in the nanomaterials, particularly for samples that were subjected to a longer annealing duration of 3.40 hrs. Based on this finding, it appears that the nanomaterials display a significant degree of transparency in both the

visible and infrared areas of the electromagnetic spectrum.

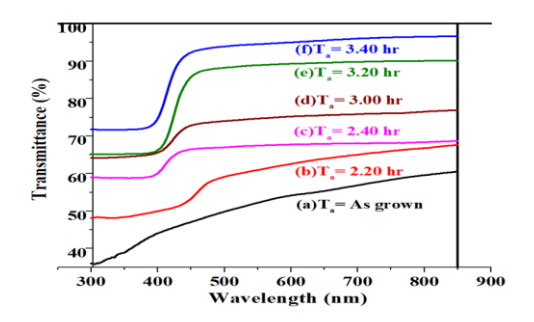


**Figure** (5) The transmittance spectrum of AZO nanofilms annealed with different annealing times.

This work suggests that the reduction in thermal concentration of crystalline nanomaterials at elevated temperatures leads to an increase in the transmittance of annealed AZO films with extended annealing durations. The indicates an increase graph transmittance with rising in the annealing time for all curves, and also increasing in transmittance increasing wavelength in a single sample. It was observed that when the annealing duration increased, the average optical transmittance also increased, confirming the researcher's findings. [32,33].

## 3.4.3 Optical Energy Gap (Egop)

The optical energy gap of the direct transition was calculated by using Tauc relation. The present work established that the optical energy gap of the AZO nanostructures, subsequently annealed for varying durations (0.00, 2.20, 2.40, 3.00, 3.20, 3.40) hr at 500°C, diminishes with prolonged annealing time.

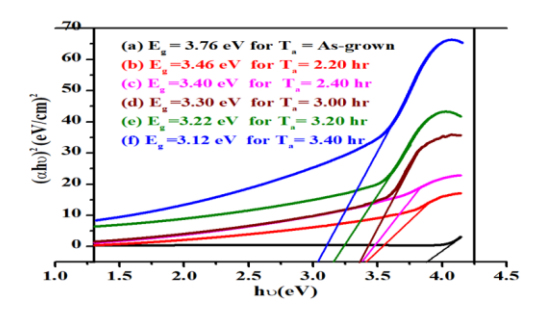


**Figure (6)** The change in the energy gap values for AZO Nano films at different annealing times

Extrapolating the straight line of  $(\alpha h \nu)^2$  against the photon energy  $(h \nu)$ , as illustrated in Figure (6), yields the optical energy gap, with  $(\alpha h \nu)^2$  serving as a function of the photon energy. With an increase in the annealing duration, a reduction in the optical energy gap for all samples was noted. This effect is associated with the gradual increase in particle size that occurs throughout the annealing process. These results align with the conclusions drawn by the researcher. [33,34].

Figure (6) illustrates that the optical energy gap in the blue spectrum region shifts following the annealing of samples at 500 °C for 2.20 hrs, concurring with the energy gap of the red region as annealing progresses. A band gap was identified, increasing to (3.46 eV) and subsequently decreasing to (3.12 eV) with extended annealing time up to 3.40 hrs, as detailed in Table (2). Researches indicate that the tail of the band results from defects, including the existence of holes and surface roughness, which contribute to a decrease in the energy gap as the unsaturated defects progressively stabilize during thermal annealing. In addition, this results in a decrease in the number of unsaturated defects, which is accompanied by an increase in the

quantity of saturated bonds and a decrease in the density of local states within the band structure [30, 34, 35].

It is posited that numerous defects were generated throughout the crystal development process, and these defects can be eliminated through annealing, commencing at a duration of 2.20 hr at a temperature of 500°C. This improves the crystallization quality of the resultant materials by reducing defects in the (AZO) nanomaterials with prolonged annealing time, causing the energy gap to shift towards the red, thereby resulting in the optical range edge to shift to red due to increased concentration. [19].

## 3.4.4 Extinction Coefficient (k)

The extinction coefficient was determined for all unannealed and annealed AZO nanofilms with varying annealing durations, and it can be derived using equation (2).

$$k = \alpha \lambda / 4\pi$$
 (3)

The absorption coefficient is denoted by  $\alpha$ , while the wavelength is represented by  $\lambda$ . Figure. 7 illustrates the extinction coefficient's variation with respect to the wavelength ( $\lambda$ ) for annealed AZO nanofilms with variable annealing durations within the 300-850 nm range. For each curve, it has been shown that the extinction coefficient increases as the wavelength increases,

and that the extinction coefficient of the samples decreases as the annealing time increases. It was observed that for all samples, the extinction coefficient is start elevating in the high ultraviolet region, with less down in the range (325-350) nm, and then in the low visible region subsequently increases again for the high visible region and above, that is agreed with the findings of the researcher [36].

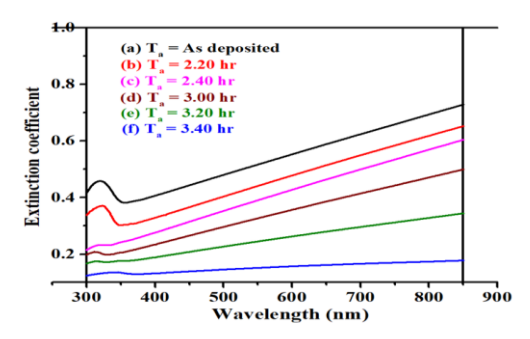


**Figure (7)** The extinction coefficient for AZO nano films as a function of wavelength at different annealing times

## 3.4.5 Refractive Index

Equation (3) was employed to ascertain the refractive index (n) of the AZO nano coatings.

$$n = \left[\frac{4R}{(R-1)^2} - k_0^2\right]^{\frac{1}{2}} - \frac{(R+1)}{(R-1)}$$
 (4)

The reflectance is denoted by R, while the extinction coefficient is represented by k. Figure (8) illustrates the refractive indices of AZO nano films samples that were deposited on glass substrates, which vary with wavelength and different annealing times, indicating the velocity of light traversing a certain medium. The refractive indices of the materials vary with annealing time and the enhancement of nanostructure crystallization, as evidenced by XRD and the density quality of the nanomaterial composition. The refractive index increases with increased of annealing time, from (0.00 - 3.40) hr, for all sample curves, and it's reduced with increased the wavelength. At (0.00) hr, the refractive index values decrease with increasing wavelength, ranging from (2.31) to (1.75) in the UV region, from (1.75) to (1.25) in the VIS region, and from (1.25) to (1.12) in the NIR region for the unannealed sample (black curve). In the ultraviolet (UV) region, the range extends from (2.27) to (2.24), while in the visible light region (VIS), it extends from (2.24) to (1.77),subsequently rising to (1.85) in the near-infrared region (NIR) for the sample (3.40hr) represented by the blue curve. Our findings indicate that an increase in annealing time correlates with a rise in the refractive coefficient, supporting the notion that annealing the reflection enhances nanomaterials. The elevated oxygen ratio may contribute to the high refractive of index (AZO) nanomaterials; specifically, with increased annealing time results in increased oxygen concentration for the (AZO) samples, thereby elevating the refractive index. This observation aligns with the findings obtained by Herve and Vandamm, who noted that a reduction in the energy gap value corresponds to an increase in the refractive index value [37].

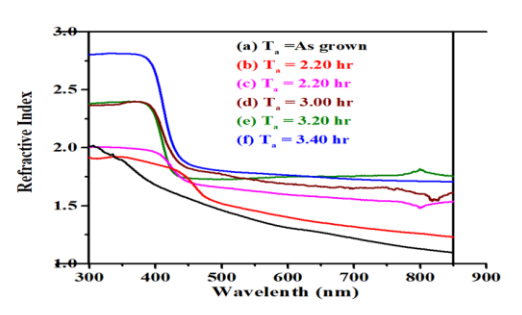


**Figure (8)** The refractive index as a function to the wavelength for the (AZO) nano films annealed with different annealing times.

#### **Conclusion:**

The samples of AZO nano films prepared using the technique (sol gel and spin coating) of post-annealing for different times while keeping the annealing temperature constant (500°C) compared to other non-annealed samples, led to a change in the structural, morphological and optical properties. In this study, the effects of annealing duration on surface as evidenced by XRD, SEM and EDX. The XRD findings demonstrate that each film has an unique AZOhexagonal crystal structure with a preferred orientation. With longer annealing times, the crystallite size rose from 15 nm to 34 nm. In AZO, optical transitions occur directly, and the value of the optical energy gap reduces as annealing time is increased. With the longer annealing times. transmittances increase from 63% to 91%. Despite the post-deposition heat treatments, the annealing effect was seen on the optical properties as a moderate decrease in Eg from 3.76 eV to 3.12 eV at low transmittance values (92%).

#### **References:**

[1] Applerot G., Lipovsky A., Dror R., Perkes N., Nitzan Y., Lubart R. and Gedanken A., "Enhanced antibacterial activity of nanocrystalline ZnO due to increased ROS mediated cell injury", Advanced Functional Materials, (2009), Vol. 19, PP.842 852.

- [2] Hu S-H, Chen Y-C, Hwong C-C, Peng C-H, Gong D-C, "Development of a wet chemical method for the synthesis of arrayed ZnO Nano rods", Journal of Alloys and Compounds, Vol. 500, (2010), PP. 117-121.
- [3] Boukhicha R. Charpentier C. Prod'Homme P. P. Roca i Cabarrocas, J. Lerat, T. Emeraud, E. Johnson. "Influence of sputtering conditions on the optical and electrical properties of laser-annealed and wet-etched room temperature sputtered ZnO:Al thin films," Thin Solid Films, No. 555 (2014), pp. 13–17.
- [4] Herna G., A. Vega, I, Juarez, J. Camacho, O. Are's, V. Rejon, J. Pen and G. Oskam. "Effect of a compact ZnO interlayer on the performance of ZnO-baase dye-ensitized solar cells", Solar Energy Materials, No. 100 (2012) pp. 21-26.-
- [5] Torchani A, S. Saadaoui, R. Gharbi and M. Fathallah. "Sensitized solar cells based on natural dyes", Current Applied Physics 15 (2015) pp. 307-312.
- [6] Ayouchi, R., et al. "Preparation and characterization of transparent ZnO thin films obtained by spray pyrolysis." Thin solid films 426.1-2 (2003): 68-77.
- [7] Ma J, Ji F, Zhang D H, Ma H L, Li S Y. Optical and electronic properties of transparent conducting ZnO and ZnO:Al films prepared by evaporating method. Thin Solid Films (1999); 357: 98–101.
- [8] Jianhua Hu, and Roy G. Gordon. "Textured aluminum-doped zinc oxide thin films from atmospheric

- pressure chemical-vapor deposition." Journal of Applied Physics 71.2 (1992): 880-890.
- [9] Mass J, Bhattacharya P, Katiyar R S. Analysis of microstructures using the ion acoustic effect. Mater. Sci. Eng. B (2003); 103: 9–11.
- [10] Ko H D, Tai W P, Kim K C, Kim S H, Suh S J, Kim Y S. Properties of Si-rich SiO2 films by RF magnetron sputtering. J. Cryst. Growth (2005); 277: 352–356.
- [11] Nunes P, Malik A, Fernandes B, Fortunato E, Vilarinho P, Martins R. Influence of the doping and annealing atmosphere on zinc oxide thin films deposited by spray pyrolysis. Vacuum (1999); 52: 45–49.
- [12] Musat V, Teixeira B, Fortunato E, Monteiro R C C, Vilarinho P. Al-doped ZnO thin films by sol-gel method. Surf. Coat. Tech. (2004); 180/181: 659–662.
- [13] Wang Y G, Lau S P, Lee H W, Yu S F, Tay B K, Zhang X H, Hing H H. Photoluminescence study of ZnO films prepared by thermal oxidation of Zn metallic films in air. J. Appl. Phys. (2003); 94: 354–358.
- [14] Cho J, Nah J, Oh M S, Song J H, Yoon K H, Jung H J, Choi W K. Enhancement of Photoluminescence and Electrical Properties of Ga-Doped ZnO Thin Film Grown on -Al2O3(0001) Single-Crystal Substrate by rf Magnetron Sputtering through Rapid Thermal Annealing. Jpn. J. Appl. Phys. (2001); 40: L1040–L1043.
- [15] Ozaki K, Gomi M. Strong Ultraviolet Photoluminescence in Polycrystalline ZnO Sputtered Films.

- Jpn. J. Appl. Phys. Part 1 (2002); 41: 5614–5617.
- [16] Ogata K, Sakurai K, Fujita Sz, Fujita Sg, Matsushige K. Effects of thermal annealing of ZnO layers grown by MBE. J. Cryst. Growth (2000); 214/215: 312–315.
- [17] Taunk P.B., R. Das, D.P. Bisen, R.K. Tamrakar, Nootan Rathor, "Synthesis and optical properties of chemical bath deposited ZnO thin film", Karbala International Journal of Modern Science Vol.1, No.3, p.p. 159-165, (2017).
- [18] Al-Asedy, H. J., Ati, A. A., Bidin, N., & Lee, S. L... "ZnO QDs Deposited on Si by Sol-Gel Method: Role of Annealing Temperature on Structural and Optical Properties." Modern Applied Science 10.4 (2016): 12-20.
- [19] Shu-Wen, Xue. "A Study of annealing time effects on the properties of Al: ZnO." Physics Procedia 25 (2012): 345-349.
- [20] Abbas, K. N., Bidin, N., Sabry, R. S., Al-Asedy, H. J., Al-Azawi, M. A., & Islam, S. "Structures and emission features of high-density ZnO micro/nanostructure grown by an easy hydrothermal method." Materials Chemistry and Physics 182 (2016): 298-307.
- [21] Baruah, Sunandan, a.nd Joydeep Dutta. "Hydrothermal growth of ZnO nanostructures." Science and technology of advanced materials (2009).
- [22] Malek, M. F., Mamat, M. H., Musa, M. Z., Khusaimi, Z., Sahdan, M. Z., Suriani, A. B., ... & Rusop, M.

- "Thermal annealing-induced formation of ZnO nanoparticles: Minimum strain and stress ameliorate preferred c axis orientation and crystal-growth properties." Journal of alloys and compounds 610 (2014).
- [23] Qaseem, S., Naeem, M., Ikram, M., & Zahra, R. "The effect of annealing time and gas flow rate on optical and magnetic properties of (Al, Co) co-doped ZnO nanoparticles by varying Al concentration." JOURNAL OF NANOSCOPE (JN) 2.1, (2021).
- [24] Kurtaran, Sema. "Al doped ZnO thin films obtained by spray pyrolysis technique: influence of different annealing time." Optical Materials 114. (2021).
- [25] Vanaja, A., G. V. Ramaraju, and K. Srinivasa Rao. "Structural and optical investigation of Al doped ZnO nanoparticles synthesized by sol-gel process." Indian Journal of Science and Technology 9.12 (2016): 87013.
- [26] Lin, Y., et al. "Green luminescent zinc oxide films prepared by polymer-assisted deposition with rapid thermal process." Thin Solid Films 492.1-2 (2005): 101-104.
- [27] Pearton, S. J., et al. "Recent progress in processing and properties of ZnO." Superlattices and Microstructures 34.1-2 (2003): 3-32.
- [28] Motloung, Setumo Victor, et al. "Effects of annealing time on the structure and optical properties of ZnAl2O4/ZnO prepared via citrate solgel process." Materials Today Communications 14 (2018): 294-301.
- [29] Siregar, Nurdin, and Johnny Panggabean. "The effect of post

- annealing time on structural and optical properties of ZnO thin films by sol-gel spin coating method." Journal of Physics: Conference Series. Vol. 1428. No. 1. IOP Publishing, (2020).
- [30] Soliman, L. I., M. E. Sayed, and N. F. Osman. "Dependence of Structural and Optical Properties on Annealing Time of ZnO Nano-Structure." (2022).
- [31] Ismail, Raid A., Nadir F. Habubi, and Hussam R. Abid. "Effect of annealing temperature on the optical properties of ZnO nanoparticles." International Letters of Chemistry, Physics and Astronomy 4 (2014).
- [32] Abdelghani, Ghazouan Mahmood, Ali Ben Ahmed, and Aseel Basim Al-Zubaidi. "Synthesis, characterization, and the influence of energy of irradiation on optical properties of ZnO nanostructures." Scientific Reports 12.1 (2022): 20016.
- [33] Bhunia, A. K., S. S. Pradhan, and S. Saha. "Effect of annealing time on the optical and structural properties of ZnO nanorods." (2019).
- [34] Özütok, Fatma, and Emin Yakar. "Annealing time effect on the optical properties of Zn (O, OH, S) films onto ZnO seed layer under unvacuum ambient." Sakarya University Journal of Science 22.6 (2018): 1704-1710.
- [35] Sadananda Kumar, N., Kasturi V. Bangera, and G. K. Shivakumar. "Effect of annealing on the properties of zinc oxide nanofiber thin films grown

by spray pyrolysis technique." Applied Nanoscience 4 (2014): 209-216.

- [36] Moreh, A. U., et al. "The role of annealing temperature on optical properties of ZnO thin films prepared by spray pyrolysis techniques." (2015).
- [37] Herve, P., and L. K. J. Vandamme. "General relation between refractive index and energy gap in semiconductors." Infrared physics & technology 35.4 (1994): 609-615.